Journal of
APPLIED
BIOMEDICINE

J Appl Biomed. **11**: 235–242, 2013
DOI 10.2478/v10136-012-0042-7
ISSN 1214-0287

ORIGINAL ARTICLE

Effects of therapeutic ultrasound on the nuclear envelope and nuclear pore complexes

Naděžda Vaškovicová[1, 2], Zdena Druckmüllerová[3], Roman Janisch[4], Jiřina Škorpíková[1], Vojtěch Mornstein[1]

[1]Department of Biophysics, Faculty of Medicine, Masaryk University, Brno, Czech Republic
[2]Department of Condensed Matter Physics, Faculty of Science, Masaryk University, Brno, Czech Republic
[3]Institute of Physical Engineering, Faculty of Mechanical Engineering, Brno University of Technology, Czech Republic
[4]Department of Biology, Faculty of Medicine, Masaryk University, Brno, Czech Republic

Received 5th April 2013.
Revised 10th May 2013.
Published online 7th June 2013.

Summary
The effects of acoustic waves on membrane structures, and any resulting consequences of this treatment on membrane subunit structures, remain poorly understood, as are the principals of related clinical effects. With a focus on morphological changes in the nuclear envelope, the current study presents detailed observations of membrane structures exposed to therapeutic ultrasound. Ultrasound treatment most commonly resulted in distinct changes in the distribution of nuclear pore complexes (NPCs) and mean NPC number per unit area after 30 min of repair, as well as alterations in NPC diameters on the protoplasmic face of fractured nuclear membranes after 10 min of repair. The greatest effects of ultrasound on nuclear envelope structure and NPCs were not to appear immediately, but became evident after repair processes were initiated. Results from the current study may contribute to the general view on the biophysical effects of therapeutic ultrasound on cell morphology and, particularly, the understanding of this effect in relation to the nuclear envelope.

Key words: HL-60 cells; ultrasound biophysical effect; image analysis; nuclear pore distribution; pore diameter; freeze-etching; nuclear envelope

INTRODUCTION

Although ultrasound, as a physical factor, is frequently used in routine medicine, at the cellular level, the effects of acoustic waves on cell membranes are not fully understood. The physical properties of ultrasound are utilised in ultrasonography, while its biophysical effects on cells and tissues are used in physical therapy. The ultrasound effects on targeted tissues and potentially associated risks are known, but all cellular mechanisms induced by ultrasound have yet to be elucidated. For *in vitro* studies on stimulatory and inhibitory effects of ultrasound on cell cultures, it is particularly important to monitor the nucleus and nuclear envelope. The nuclear envelope is a complex dynamic system composed of membranes and proteins that, when treated by therapeutic ultrasound, are exposed to acoustic waves. The membrane-acoustic wave interaction results in biophysical changes in protein structures, subsequently leading to functional changes detectable by molecular biology and biophysics techniques. These changes initiate a cascade of secondary processes, eventually leading to a therapeutic result.

✉ Naděžda Vaškovicová, Department of Biophysics, Faculty of Medicine, Masaryk University, Kamenice 5, 625 00 Brno, Czech Republic
nvaskovicova@seznam.cz
☎ +420 549 492 890
+420 549 491 320

Relevant studies on the effect of therapeutic ultrasound are largely concerned with the measurement of membrane potentials (Mazzanti et al. 2001), changes in transfer of Ca^{2+} ions across the membrane (Roehring et al. 2003, Hassan et al. 2010) or nuclear envelope involvement in cell viability and proliferation (De Deyne and Kirsch-Volders 1995, Roehrig et al. 2003, Tsai et al. 2005, Bernard et al. 2008, 2010, Zhong et al. 2011). These studies describe only changes concerning functions of the nuclear envelope, such as its permeability, and little is known about changes in the morphology of membranes after exposure to therapeutic ultrasound.

Due to their complex ultrastructure, nuclear pores in this study are referred to as nuclear pore complexes (NPCs). An exact study of changes in location of NPCs is hindered by their natural uneven distribution (Rabut et al. 2004, Maeshima et al. 2006, Antonin et al. 2008), which may vary with each cell cycle phase or cell line (Maul et al. 1971, Sugie et al. 1994). Some authors have employed mathematical analysis to study NPC distribution, but these studies have dealt only with cells not previously exposed to external physical factors (Daigle et al. 2001, Hinshaw and Milligan 2003, Dultz and Ellenberg 2010). There are also reports of using cryo-electron tomography to visualise and identify the most frequently found NPCs, including their inner structure and the structure of their subunits, and to assess their size (Beck et al. 2004, 2007). Since the structures are visualised in their native fully hydrated environment, this technique is likely to provide the most accurate morphological assessments.

The current study was focused on morphological responses of cells exposed to therapeutic ultrasound. Specifically, changes in the number, distribution and size of NPCs due to acoustic energy application were investigated. Nuclear envelopes were visualised using a freeze-etching (freeze-fracturing) technique, which allows us to obtain replicas of membrane structures in relatively large areas and distinguish small protein fragments. This technique has previously been used to study nuclear envelopes in detail to identify and describe their structures (Kartenbeck et al. 1971, Maul et al. 1971, 1972, 1980, Benchimol 2004, Cavicchia et al. 2010).

Based on literature and results of our previous studies on nuclear membranes treated with therapeutic ultrasound, we focused, in the first place, on fractures through nuclear pore complexes. Due to their role in molecule transport across the nuclear envelope, as well as their complicated morphology and membrane-integrated proteins, NPCs may serve as a useful indicator of the biophysical effect of ultrasound and related repair processes.

MATERIAL AND METHODS

Cells

HL-60 (human promyelocytic leukemia) cells were maintained under standard cultivation conditions in an atmosphere of 5% carbon dioxide at a temperature of 37 °C. Cells were passaged every 3 days. The culture medium consisted of Dulbecco's minimal essential medium supplemented with 10% bovine serum, 100 µg/ml streptomycin/penicillin and 2 mM glutamine (Biotech, a. s., Prague, Czech Republic). For all experiments, cells were concentrated by spinning at 900 rpm for 5 min and resuspended in culture medium to give a final concentration of 10^7 cells per ml.

Cell exposure

A 1.5 ml aliquot of cell suspension, 10^7 cells per 1 ml of culture medium, was transferred into a polyethylene test tube, which was inserted in a holder rotating at a speed of 10 rpm. The cells were exposed to therapeutic ultrasound generated by a BTL-07p device (Beautyline Ltd., Prague, Czech Republic) at a frequency of 1 MHz and an intensity of 1 W/cm^2 in continuous mode in the horizontal near field for 10 min. The transducer head area was 4 cm^2. In a polyethylene test tube filled with distilled warm (37 °C) water, attenuation of acoustic pressure was 26% of the original value. Acoustic pressure was controlled by a calibrated PVDF hydrophone, type MH28-6 (Force Institute, Copenhagen, Denmark). Distilled water warmed to 37 °C provided a contact medium.

Cell processing

A suspension of cells treated by ultrasound was placed in a 37 °C water bath along with a suspension of control (untreated) cells. To test the degree of nuclear envelope repair, samples from both suspensions were collected at 0 min, 10 min, 20 min, 30 min, 60 min and 120 min after treatment and fixed for 10 min in fixation solution (2% paraformaldehyde and 2.5% glutaraldehyde in 0.1 M cacodylate buffer) at room temperature. After washing with 0.1 M cacodylate buffer, fixed cells were resuspended in 20% (w) glycerol and then stored in a refrigerator at 6 to 7 °C overnight until use.

Freeze-etching

A drop of dense cell suspension was placed onto a gold carrier and deep frozen in melting nitrogen at –210 °C. In a BAL-TEC 060 Freeze-Etching System (Leica) specimens were fractured and shadowed with a platinum and a carbon layer at 45° and 90° angles, respectively (vacuum, 10^{-5} Pa; temperature,

–100 °C). Organic matter was removed with 75% sulphuric acid, and a metal replica of exposed cell structures was obtained. After rinsing with distilled water, the replica was placed onto a copper grid. Replicas were examined using a MORGAGNI 268D (FEI) transmission electron microscope, and fracture faces of the inner and outer membranes of the nuclear envelope were photographed. The designation in figures was used as described by Speth and Wunderlich (1970) and Kartenbeck et al. (1971).

Image analysis

The action of ultrasound on the nuclear envelope was assessed in micrographs by means of three different parameters: membrane-per-pore area, number of NPCs per unit area and diameter of NPC.

The assessment of changes in NPC distribution was based on determining variations in the size of a nuclear membrane area belonging to one NPC. In electron micrographs of nuclear envelopes (36,000× magnification), individual NPCs were manually marked using the Adaptive Control Contrast (ACC) program (Fig. 1A), and the coordinates (x, y) of each NPC centre were determined. Using these, boundaries between each two neighbouring NPCs were delineated (Fig. 1B). Areas of the nuclear membrane, each belonging to one NPC, i.e., membrane-per-pore (MPP) area, were evaluated using Voronoi tessellation (Jackson et al. 1999, Frank and Hart 2008, Sung and Yethiraj 2008). Areas at the edges of the micrograph that had poorly defined boundaries, as well as membrane areas that appeared concave or convex in relation to the ideal 2D projection plane (Fig. 1B), were excluded from statistical analysis.

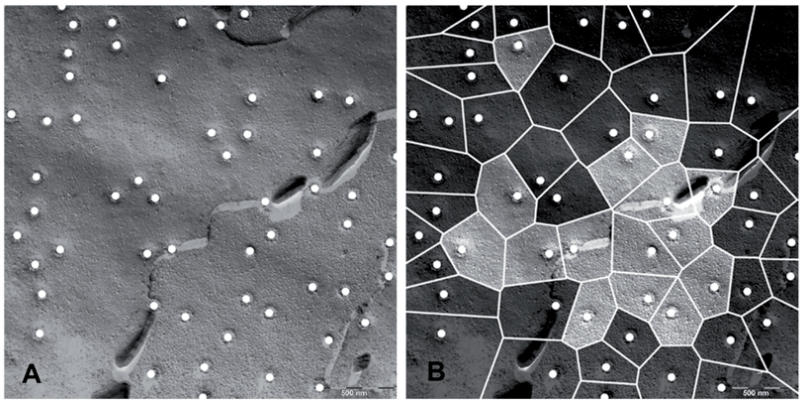

Fig. 1. **Image analysis of membrane-per-pore areas by means of the Voronoi tessellation.** *(A)* White points identify nuclear pore complex (NPC) centres. *(B)* White lines mark the boundaries of membrane-per-pore areas. Dark areas were not included in statistical analysis.

The mean number of NPCs in a sample was assessed in the same electron micrographs used for Voronoi tessellation analysis. In the nuclear membrane area lying in an ideal 2D projection plane, NPCs were manually marked and counted. Subsequently, a boundary for the region containing these NPCs was manually marked and its area was measured. For convenience, the mean number of NPCs is reported per 1 μm^2, which was designated as a unit area in this study.

Electron micrographs in which the fracture plane ran through both the inner and the outer membrane were selected, and NPC diameters on the protoplasmic and exoplasmic fracture faces were measured. NPC diameters were manually marked in the micrographs, and the protoplasmic and exoplasmic fracture faces were assessed separately.

Statistical analysis

The numbers of NPCs per unit area (1 μm^2), size of MPP areas and diameter of NPCs were expressed as mean±S.D.; the diameter and MPP area ranges were expressed as min-max. In all samples, the mean NPC number per unit area was determined in each of 50 nuclear membranes examined; the size of MPP area was assessed for 500 to 1000 membrane regions, and the diameter was measured in 250 to 800 NPCs found on the protoplasmic and exoplasmic fracture faces of the inner or the outer nuclear membrane.

The results of NPCs per unit area, Voronoi tessellation analysis and NPC diameter measurements at the defined intervals were compared between ultrasound-treated and untreated samples and evaluated using the two-sided Mann-Whitney U-test at the significance level $2\alpha = 0.05$ (STATISTICA 10 software).

RESULTS

Ultrasound-treated and untreated cells were compared based on the following parameters: mean number of NPCs per unit area, NPC distribution in terms of the size of MPP area, and variation in NPC diameters. Changes in NPC numbers per unit area relative to repair period are shown in Table 1.

Table 1. **The mean number of nuclear pore complexes (NPCs) per unit membrane area assessed at defined intervals.**

Number of NPCs per unit area (1 μm^2)	Repair/incubation time (min)					
	0	10	20	30	60	120
Control sample	9.3±1.6	9.0±1.2	9.1±1.5	9.2±1.2	9.0±1.2	9.6±1.4
Ultrasound-treated sample	8.5±1.3*	8.3±1.3*	7.4±0.3*	7.6±1.2*	7.0±2.0*	9.4±1.3

50 nuclear envelopes were evaluated in each sample; 36,000× magnification. * Statistically significant as compared with controls.

The effect of therapeutic ultrasound on pore distribution was evaluated based on changes in sizes of MPP areas. A significant difference in size of MPP areas between the treated and untreated samples was apparent immediately after ultrasound treatment (0 min). The mean of MPP areas in treated sample was 0.13±0.05 μm^2 and in control sample it was 0.11±0.04 μm^2. A significant difference was also found 30 min after the treatment. In the ultrasound-treated sample, variance in MPP areas increased. The mean value of MPP areas in ultrasound-treated sample was 0.14±0.07 μm^2, in control sample 0.11±0.04 μm^2, with the range of values in treated sample 0.04–0.67 μm^2 and 0.03–0.29 μm^2 in control sample. At 60 min there was still a significant difference in MPP areas, but the range was similar in both treated and untreated samples (0.03–0.29 μm^2). At 120 min there was no significant difference in MPP areas between treated and untreated samples.

For assessment of the effect of ultrasound treatment on the size of NPCs, mean NPC diameters on the protoplasmic fracture faces were compared

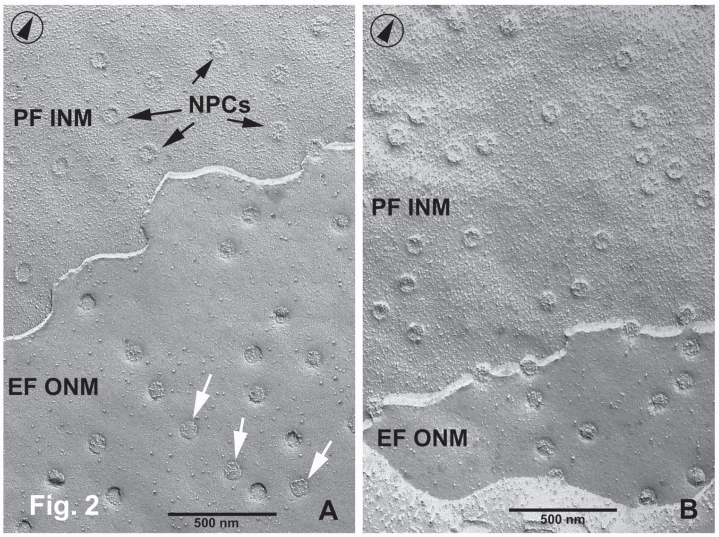

Fig. 2. **Fractured nuclear membranes.** *(A)* specimen treated by ultrasound at a frequency of 1 MHz and an intensity of 1 W/cm^2 for 10 min; *(B)* control specimen; both fixed at 0 min. PF, protoplasmic fracture face; EF, exoplasmic fracture face; INM, inner nuclear membrane; ONM, outer nuclear membrane. Nuclear pore complexes (NPCs) on the PF of the inner membrane were similar in appearance in both specimens but, in the treated one (black arrows), NPCs appear to be nearly level with the membrane surface. NPCs on the EF of the outer membrane in the treated specimen were different in appearance (white arrows) due to protein fragments incorporated into the outer nuclear membrane. Encircled black arrows indicate the direction of platinum shadowing. Bar, 500 nm.

with those on the exoplasmic fracture faces, ranging from 0.3–4.2 nm and 1.3–5.0 nm in treated and untreated samples, respectively.

Immediately following ultrasound treatment (0 min), there was a significant difference in NPC diameters on the protoplasmic fracture face in treated samples as compared with the control. In treated sample, diameter variability was greater and the mean of NPC diameter (89±4 nm) was higher by 6 nm in comparison with the control. At 10 and 20 min differences in both the size and shape of NPCs were still significant and, at 10 min, the mean of diameter was 94±4 nm in treated sample and 83±4 nm in control sample; at 20 min the respective means were 96±4 nm and 86±5 nm. At 30 min this difference was no longer significant. On the exoplasmic fracture face, significant differences in NPC diameters between treated and untreated samples were observed at 0 min and the difference between means of diameters was 5 nm (diameter of NPC in treated sample 89±5 nm).

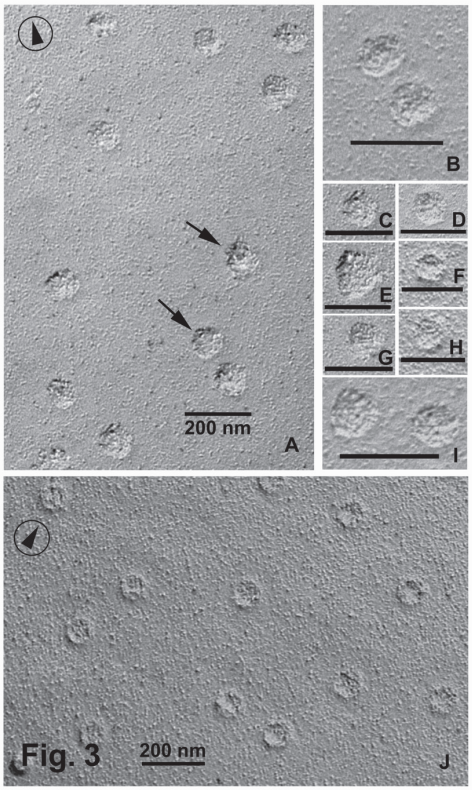

Fig. 3. **Electron micrographs of protoplasmic fracture faces.** Specimens fixed at 10 min: *(A–I)* examples of varied nuclear pore complex (NPC) morphology on protoplasmic fracture faces of the nuclear membrane treated by ultrasound; *(J)* control membrane. Black arrows indicate enlarged and deformed shapes of fractured NPCs. Sections B to I come from different nuclear envelopes. Encircled black arrows show the direction of platinum shadowing. Bar, 200 nm.

Upon comparison of the micrographs of fracture faces of the inner and outer nuclear membranes, the protoplasmic fracture face of the inner membrane in treated samples showed fragments of membrane proteins, and its NPCs were more deeply immersed in the membrane surface than those in the control sample (Fig. 2 and 3). In one area of the exoplasmic fracture face of the outer membrane, the characteristics of fracture through NPCs were different from those in the control sample (Fig. 2A). Differences in NPC appearance on the protoplasmic fracture face between treated and untreated samples at 10 min are shown in Fig. 3 A–I.

DISCUSSION

Morphological alterations in the nuclear envelope, involving changes in the number or distribution of NPCs, in response to physical factors, such as temperature or acoustic oscillations, are poorly understood (Baker et al. 2001, Cambier et al. 2001). This is due to the fact that distribution of NPCs naturally varies in the nuclear envelope from cell to cell (Rabut et al. 2004, Maeshima et al. 2006, Antonin et al. 2008). Furthermore, available imaging methods require sample preparation procedures that have a tendency to damage structures of interest and create artefacts.

A morphological description of the structure of protein complexes integrated into membranes is difficult and tedious. Freeze-etching provides exact metal replicas of membrane structures and allows for detailed visual analysis of specimens which are not subject to ongoing changes during examination or to destruction. Replicas of cells reveal details on fracture faces of the nuclear envelope, such as protein fragments incorporated into the membrane. This technique also enables us to study the distribution of proteins, i.e., pores or pore complexes, on the membrane surface and evaluate changes in their characteristics (Moor and Mühlethaler 1963, Kartenbeck et al. 1971, Maul et al. 1971, 1972, 1980, Cavicchia et al. 2010, Heuser 2011).

For finding evidence of membranes being affected, use of the freeze-etching technique and dense suspension samples was preferred. HL-60 cells were employed in the current study because their morphology is well-defined, they are easy to culture and multiply rapidly, providing up to 10^6 cells per ml in one passage. Morphological cell line characteristics have been described in previous studies (Vaskovicova et al. 2006, 2009, 2011).

Acoustic oscillations applied to tissues and cell cultures exert their effect primarily on membranes

and, consequently, the protein structures integrated into the membranes (i.e. membrane-associated proteins). Owing to their complexity based on the involvement of a large number of protein subunits, NPCs can serve as an indirect indicator of any mechanical action of ultrasound on nuclear envelopes. Changes in the NPC inner structure may not be the only consequence of ultrasound effect on week chemical bonds between proteins; there are also changes in the shape and characteristics of fractures through NPCs which are due to different strength of bonds between protein subunits. Damage to subunits may result in pore disintegration, evident by altered numbers or distribution of NPCs.

Defining the size of a membrane area belonging to one NPC is a key factor in the assessment of NPC distribution throughout the nuclear envelope. The size of an MPP area is equivalent to the distance between neighbouring NPCs, which is distinct from the number of NPCs found in a unit area. While the same number of NPCs can be found in a unit area of both a treated and an untreated membrane, the distribution of NPCs in them may be completely different. Assessing size of MPP area in combination with counting NPCs per unit area allowed us to gain a deeper insight into morphological changes in the nuclear envelope following exposure to ultrasound.

The freeze-etching method can only visualise NPCs whose subunits are incorporated into the inner or outer membranes of the nuclear envelope (Lenz-Böhme et al. 1997, Lim et al. 2008, Fernandez-Martinez 2009, Doucet and Hetzer 2010). It has been suggested that a decrease in the mean number of NPCs per unit area implies disintegration of some NPCs. Consistently with this assumption, a decrease in the mean NPC number per unit area was observed 30 and 60 min after ultrasound exposure. Similarly, on the assumption that the size of the nuclear membrane remains unchanged after treatment, variability in MPP areas in the treated samples markedly increased as compared with the control samples examined at the same time intervals. This increased variability as well as a greater range result from dividing the MPP area of the missing NPC amongst the neighbouring NPCs.

Any NPC requires a certain time for its relocation or re-assembly (Bucci and Wente 1997, Dultz and Ellenberg 2010); this involves several hours and varies with each cell line and the proliferative capacity of its cells. After allowing 120 min for repair, the mean of NPC number per unit area and also MPP area variability were comparable in both treated and untreated samples, indicating that cells exposed to ultrasound were able to restore the initial characteristics of their nuclear envelopes in culture medium at a temperature of 37 °C during 120 min.

Studies using cryo-electron tomography or mathematical modelling of NPC shape and size have suggested that NPC diameter can be measured on either the inner or the outer nuclear membrane since the cytoplasmic ring and the nuclear ring have equal diameters (Hinshaw and Milligan 2003, Beck et al. 2004, 2007). NPC diameters reported in this study were obtained from measuring the protoplasmic and cytoplasmic fracture faces of the inner and outer nuclear membranes. As such, these values cannot be compared with those of the cytoplasmic and nuclear rings assessed by cryo-electron tomography. The appearance of the ring of a fractured NPC seen on the protoplasmic fracture face is, in addition to protein fragments integrated into the membrane, due to the presence of protein and porine fragments derived from a spoke ring of this NPC. In an NPC ring on the exoplasmic fracture face, the appearance also involves protein fragments coming from the protoplasmic or the nuclear ring and partly also from the spoke ring, in addition to membrane-incorporated proteins. Thus, the shape and size of any NPC ring on the protoplasmic or exoplasmic fracture face varied in relation to the true size of this NPC as well as to the involvement of fractured protein subunits derived from some of the rings mentioned above (Kartenbeck et al. 1971). When bonds among membrane proteins were disrupted by ultrasound waves, the spoke, cytoplasmic and nuclear rings were fractured differently, resulting in an altered size or deformation of the usually circular NPC.

A significant difference in NPC diameters on the protoplasmic fracture face was observed immediately after ultrasound treatment and lasted up to 30 min, with the most significant difference being at 10 min after treatment. On the exoplasmic fracture face, the most significant differences were seen at 0 min, thus providing further evidence that ultrasound primarily disturbs protein subunits of the spoke ring, resulting in significant changes in NPC diameters immediately after ultrasound treatment, and lasting up to 30 min that were evident on the protoplasmic fracture face.

Although the control sample was not affected by ultrasound, gradually enlarging diameters of NPCs fractured in the protoplasmic face of the nuclear envelope were recorded. The mean of diameter increased after 20 min from the initial 83±4 nm to 86±5 nm. This can be explained, for instance, due to transport of macromolecules through NPCs which may become more frequent due to repair processes induced by manipulation with the sample before the experimental treatment. The cell suspension had to be concentrated by centrifugation and was also subjected to a short-term thermal shock. This manipulation stress can cause cell reactions or may increase cell

sensitivity to the following treatment, but its complete elimination is not possible. A detailed explanation of this stress is out of the scope of our study. Although the mean of NPC diameter in the control sample increased, in the treated sample its value was higher by 6 nm at 0 min, by 11 nm at 10 min, and by 10 nm at 20 min as compared with the control sample. Hence, these values can be taken as evidence of ultrasound-induced changes.

Changes in NPC inner structure described here are in agreement with previously reported findings of altered permeability of nuclear envelopes to large and electrically-charged molecules during and after exposure to ultrasound (Bernard et al. 2008, 2010). Such alterations may also provide an explanation of the fact that it is easier for these molecules to penetrate through the envelope during or shortly after ultrasound application. Studies on penetration of anti-cancer agents into the nucleus have shown that administration of a drug simultaneously with ultrasound application may enhance inhibitory effects of the drug and eliminate more tumour cells compared to administration of the drug alone. Therefore, augmentation of any drug delivery by simultaneous application of ultrasound may be used to improve drug efficiency, as well as to stimulate cell proliferation during healing processes in clinical practice.

ACKNOWLEDGEMENTS

The study was supported by grants 305/05/2030/S and 301/03/H005 from the Grant Agency of the Czech Republic. The authors thank Mrs. S. Modrová, Department of Biophysics, for her help with the experimental part of the study.

REFERENCES

Antonin W, Ellenberg J, Dultz E. Nuclear pore complex assembly through the cell cycle: regulation and membrane organization. FEBS Lett. 582: 2004–2016, 2008.

Baker KB, Robertson VJ, Duck FA. A Review of therapeutic ultrasound: biophysical effects. Phys Ther. 81: 1351–1358, 2001.

Beck M, Förster F, Ecke M, Plitzko JM, Melchior F, Gerisch G, Baumeister W, Medalia O. Nuclear pore complex structure and dynamics revealed by cryoelectron tomography. Science. 306: 1387–1390, 2004.

Beck M, Lucić F, Baumeister W, Medalia O. Snapshots of nuclear pore complexes in action captured by cryo-electron tomography. Nature Letters. 449: 611–615, 2007.

Benchimol M. Giardia Lamblia: behavior of the nuclear envelope. Parasitol Res. 94: 254–264, 2004.

Bernard V, Škorpíková J, Mornstein V. The combined effect of ultrasound exposure and cisplatin on human ovarian carcinoma cells A2780. Folia Biol (Praha). 54: 97–101, 2008.

Bernard V, Škorpíková J, Mornstein V, Slaninová I. Biological effects of combined ultrasound and cisplatin treatment on ovarian carcinoma cells. Ultrasonics. 50: 357–362, 2010.

Bucci M, Wente SR. *In vivo* dynamics of nuclear pore complexes in yeast. J Cell Biol. 136: 1185–1199, 1997.

Cambier D, D'Herde K, Witvrouw E, Beck M, Soenens S, Vanderstraeten. Therapeutic ultrasound: temperature increase at different depths by different modes in a human cadaver. J Rehab Med. 33: 212–215, 2001.

Cavicchia JC, Guembe G, Fóscolo M. Nuclear pores in luteal cells during pregnancy and after parturition and pup removal in the rat. A freeze-fracture study. Biocell. 34: 81–89, 2010.

Daigle N, Beaudouin J, Hartnell L, Imreh G, Hallberg E, Lippincott-Schwartz J, Ellenberg J. Nuclear pore complexes form immobile network and have a very low turnover in live mammalian cells. J Cell Biol. 154: 71–84, 2001.

De Deyne PG, Kirsch-Volders M. *In vitro* effects of therapeutic ultrasound on the nucleus of human fibroblasts. Phys Ther. 75: 629–634, 1995.

Doucet CHM, Hetzer MW. Nuclear pore biogenesis into an intact nuclear envelope. Chromosoma. 119: 469–477, 2010.

Dultz E, Ellenberg J. Live imaging of single nuclear pores reveals unique assembly kinetics and mechanism in interphase. J Cell Biol. 191: 15–22, 2010.

Fernandez-Martinez J. Nuclear pore complex biogenesis. Curr Opin Cell Biol. 21: 603–612, 2009.

Frank NP, Hart S. A dynamical system using the Voronoï tessellation. Am Mathemat Monthly. 117: 99–112, 2010.

Hassan MA, Campbell P, Kondo T. The role of Ca^{2+} in ultrasound-elicited bioeffects: progress, perspectives and prospects. Drug Discovery Today. 15: 892–906, 2010.

Heuser JE. The origins and evolution of freeze-etch electron microscopy. J Electron Microsc. 60: 3–29, 2011.

Hinshaw JE, Milligan EA. Nuclear pore complexes exceeding eightfold rotational symmetry. J Struct Biol. 141: 259–268, 2003.

Jackson NM, Jafferali R, Bell DJ, Davies GA. A study of the structure of micro and ultrafiltration membranes: the Voronoi tessellation as a stochastic model to simulate the structure. J Membr Sci. 162: 23–43, 1999.

Kartenbeck J, Zentgraf H, Scheer U, Franke WW. The nuclear envelope in freeze-etching. Springer-Verlag, Berlin, Heidelberg, New York, 1971.

Lenz-Böhme B, Wismar J, Fuchs S, Reifegerste R, Buchner E, Betz H, Schimitt B. Insertional mutation of the Drosophila nuclear lamin Dm0 gene results in defective nuclear envelopes, clustering of nuclear pore complexes, and accumulation of annulate lamellae. J Cell Biol. 137: 1001–1016, 1997.

Lim RYH, Aebi U, Fahrenkrog B. Towards reconciling structure and function in the nuclear pore complex. Histochem Cell Boil. 129: 105–116, 2008.

Maeshima K, Yamata K, Sasaki Y, Nakatomi R, Tachibana T, Hashikawa T, Imamoto F, Imamoto N. Cell-cycle-dependent dynamics of nuclear pores: pore-free islands and lamins. J Cell Biol. 119: 4442–4451, 2006.

Maul GG, Price JW, Lieberman MW. Formation and distribution of nuclear pore complexes in interphase. J Cell Biol. 51: 405–418, 1971.

Maul GG, Maul HM, Scogna JE, Lieberman MW, Stein GS, Hsu BY, Borun TW. Time sequence of nuclear pore formation in phytohemagglutinin-stimulated lymphocytes and in HeLa cells during the cell cycle. J Cell Biol. 55: 433–447, 1972.

Maul GG, Deaven LL, Freed JJ. Investigation of the determinant of nuclear pore number. Cytogen Cell Gen. 26: 175–190, 1980.

Mazzanti M, Bustamante JO, Oberleithner H. Electrical dimension of the nuclear envelope. Physiol Rev. 81: 1–19, 2001.

Moor H, Mühlethaler K. Fine structure in frozen-etched yeast cells. J Cell Biol. 17: 609–628, 1963.

Rabut G, Lénárt P, Ellenberg J. Dynamics of nuclear pore complex organization through the cell cycle. Curr Opin Cell Biol. 16: 314–321, 2004.

Roehrig S, Tabbert A, Ferrando-May E. *In vitro* measurement of nuclear permeability changes in apoptosis. Anal Biochem. 318: 244–253, 2003.

Speth V, Wunderlich F. The macronuclear envelope of Tetrahymena pyriformis GL in different physiological states. J Cell Biol. 47: 772–777, 1970.

Sugie S, Yoshimi N, Tanaka T, Mori H, Williams GM. Alterations of nuclear pores in preneoplastic and neoplastic rat liver lesions induced by 2-acytylaminofluorene. Carcinogen. 15: 95–98, 1994.

Sung BJ, Yethiraj A. Lateral diffusion of proteins in the plasma membrane: spatial tessellation and percolation theory. J Phys Chem B. 112: 143–149, 2008.

Tsai WC, Hsu CC, Tang FT, Chou SW, Chen YJ, Pang JH. Ultrasound stimulation of tendon cell proliferation and upregulation of proliferating cell nuclear antigen. J Orthop Res. 23: 970–976, 2005.

Vaskovicova N, Skorpíkova J, Janisch R. Changes in nuclear envelope structure after exposure to ultrasound. Bratisl Lek Listy. 107: 177–178, 2006.

Vaskovicova N, Skorpikova J, Janisch R. Ultra-structural changes in the nuclear membrane during interphase and apoptosis. Mikroskopia. 47, 2009.

Vaskovicova N, Skorpikova J, Janisch R. The nuclear pore complexes changed after ultrasound exposure. XX. Biologické dny. 41, 2011.

Zhong W, Sit WH, Wan JMF, Yu AC. Sonoporation induces apoptosis and cell cycle arrest in human promyelocytic leukemia cells. Ultrasound Med Biol. 37: 2149–2159, 2011.